

FAINT STELLAR PHOTOMETRY IN CLUSTERS. I. NGC 2204 AND E3

JAY A. FROGEL

Cerro Tololo Inter-American Observatory¹

AND

BRUCE A. TWAROG²

Department of Physics and Astronomy, University of Kansas at Lawrence

Received 1982 December 10; accepted 1983 March 9

ABSTRACT

Photoelectric photometry of faint stars in the sparsely populated clusters NGC 2204 and E3 obtained with the CTIO SIT vidicon is presented and analyzed. Results indicate that the vidicon camera is a linear device over, at least, a 6 mag range capable of providing magnitudes with an accuracy comparable to that of a single channel photometry for all stars in the camera field simultaneously.

Comparison of main-sequence photometry in the old disk cluster NGC 2204 down to $M_p = 6.5$ with theoretical isochrones of appropriate composition leads to an age of $2.5 \pm 0.3 \times 10^9$ years and $(m-M)_0 = 13.1 \pm 0.2$, if $E(B-V) = 0.08$. The luminosity function of the cluster is flat over most of the main sequence. This result is consistent with previous data on NGC 2506 and NGC 2420 and suggests that the luminosity function at the faint end is dominated by tidal stripping.

Attempts to calibrate the vidicon frames with the available photometry in the globular cluster E3 proved futile; published B magnitudes for E3 appear to contain a systematic, magnitude-dependent error. If the vidicon data for E3 are placed on the same system as NGC 2204, the resulting color-magnitude diagram displays few of the anomalous features noted in previous work, though the claim for a significant population of blue stragglers in the cluster is confirmed.

Subject headings: clusters: open — luminosity function — photometry

I. INTRODUCTION

NGC 2204 is an old, moderately metal-poor, disk cluster with an apparent distance modulus greater than 13.0. The only available photometry of the cluster is that of Hawarden (1976). Hawarden's data place the cluster turnoff at $V = 15.8$, with the unevolved main sequence expected to begin at about $V = 18.5$. The photoelectric sequence extends to $V = 17.6$ but is believed to be reliable only for V less than 17.0 (Hawarden 1976).

The primary purpose of this paper is to present new observations of the faint, unevolved main sequence within NGC 2204, estimates of the distance modulus and age, and a discussion of the luminosity function of the cluster. It was decided to obtain these data with a SIT vidicon tube rather than photographic plates or conventional photoelectric photometry because of the advantage of greater quantum efficiency and linearity that a SIT vidicon holds over the former and the two-dimensional advantage that it has over the latter. Also, the CTIO SIT system has seen rather little use in the direct imaging mode, and NGC 2204 seemed to be a good candidate object on which to evaluate the performance of the system because it is a relatively uncrowded cluster, thus making no great demands on the data reduction software. Despite the low concentra-

tion class of the cluster and the small field of the SIT frames (90" on a side at the f13.5 focus of the 1.5 m), it was felt that the central regions of the cluster were rich enough in members that only a few frames would be needed to achieve the scientific objectives.

Aside from providing important information about NGC 2204 itself, these data will be useful in the construction of synthesis models of the stellar populations of galaxies. Significant sources of uncertainty in these models are the variations of bolometric luminosity and effective temperature of giant stars with age and metallicity. Most work on this problem has been confined to the metal-poor end of the scale via observations of globular clusters. Attempts have been made to calibrate the metal-rich end of the scale using observations of solar neighborhood old disk giants, but this approach suffers from significant uncertainties in the knowledge of distances, ages, and metallicities of individual stars and must rely on a more statistical approach. Observations of old (few times 10^9 yr) disk clusters can be of some value in providing the necessary information for giant stars. While ages can be estimated from the color of the main-sequence turnoff, unlike globular clusters, distance moduli to these clusters can best be obtained by main sequence fitting. There are, though, few old disk clusters for which the required data are available. The present data, then, add another cluster to this short list for which reasonably good

¹ CTIO is operated by AURA, Inc. under National Science Foundation contract AST 78-27879.

² Visiting Astronomer, CTIO.

estimates of the age, metallicity, and distance are available.

Finally, data were also obtained for the sparsely populated globular cluster E3 (van den Bergh, Demers, and Kunkel 1980, hereafter BDK), originally with the objective of calibrating the NGC 2204 frames. Although the E3 data turned out not to be useful for this objective, they produced results sufficiently different from what has been published about this cluster that they are included in the present paper.

The observational procedure and reduction of the raw vidicon frames are discussed in § II, and the photometric calibration procedure in § III. The color-magnitude ($c-m$) diagrams of the two clusters in this program will be analyzed in § IV, where the age, distance modulus, and luminosity function of NGC 2204 will be derived. A summary of the conclusions will be found in § V.

II. OBSERVATIONS AND THEIR REDUCTION

A complete discussion of the vidicon camera may be found in Atwood *et al.* (1979) and in the CTIO Observer's Manual. Briefly, the vidicon at CTIO is an RCA 4804 silicon-intensified tube which has an electrostatically focused image-intensified section with a modified S-20 photocathode. For this program, the vidicon was operated in the equilibrium mode; the target was read every 22 s and the frames were co-added on disk. Operations in this mode are designed to greatly increase the dynamic range capability of the tube in a given exposure time and to minimize departures from linearity over the entire dynamic range. The tube was cooled with dry ice and placed at the f13.5 focus of the CTIO 1.5 m reflector with no intervening optics. The pixel size was set so that a 256×256 frame covered a region of sky $90''$ on a side. Telescope focusing was done by minimizing the full width at half-maximum of the profile of a bright stellar image. Typical values of the FWHM of the profile were 4–5 pixels, or just over $1''$.

Flat field exposures were taken through the B and V filters at the beginning and end of each night by exposing on the twilight sky. These were carefully examined for the presence of any stellar image. Dark frames were also taken for each night.

Exposures in B and V were obtained for three fields in NGC 2204 and one field in E3. For NGC 2204, each frame consists of a 45 minute integration, and there are three frames each in the B and V filters. For E3, integrations times varied from 30 to 45 minutes, and there are only two frames in B , but three in V . In all cases, only one BV set of each field was taken on any given night.

All of the vidicon frames were reduced in an essentially identical manner on CTIO's Datacraft computer in La Serena. First, all of the frames were normalized to the same integration time. The dark frames were subtracted from each of the cluster field frames and the flat field frames. The cluster frames were then divided by the flat frames. A slight amount

of smoothing was done to all the frames. The details of the removal of the dark and flat fields from the cluster frames did not appear to influence in any significant way the final magnitudes of the stars. For example, it mattered little whether all of the dark and flat frames from the entire run were first averaged together and then used to reduce each night's cluster data, or if each night was treated independently of the others.

The reason for the insensitivity of the final stellar magnitudes to this part of the reduction procedure stems at least, in part, from the fact that sky values were determined (as described below) from regions immediately around *each* stellar image. For this same reason, no attempt was made to correct for whatever small amount of spatial distortion might exist in the vidicon frames. In any case, magnitude residuals for the stars used for calibration appeared to be of a purely statistical, i.e., random, nature as will be discussed in the next section. Clearly, if one were doing photometry of extended sources, effects which are of negligible importance in the present instance would have to be carefully allowed for. These effects include a nonlinear dependence of the dark count on time.

All stellar images which were judged to be measurable on at least two frames in a given color were selected. In fact, nearly all images were measurable on all frames of a given field. Because of the relatively low star density in both objects, it was not necessary to employ complicated algorithms to obtain instrumental magnitudes. First, the center of each image on each frame was found and all the light in a circular "aperture" was measured. Generally, a $4''.2$ diameter aperture was used for NGC 2204 and a $2''.8$ aperture adopted for E3. In instances where crowding was a problem, a $2''.1$ aperture was used. The appropriate sky value for each star was determined by averaging over an annulus surrounding the measuring aperture and subtracted from the stellar measure. An aperture calibration was determined for each frame as necessary by measuring several dozen stars through a number of apertures. A typical dispersion in this calibration for a single measurement was ± 0.04 mag or less, independent of which apertures were used. No significant dependence on stellar magnitudes was found for the aperture calibration down to the faintest image measured.

III. CALIBRATION OF THE FRAMES

Ideally, one would like a standard star sequence with a range in color and magnitude comparable to that of the program stars and located close enough together in the sky so that the entire sequence can be imaged on one vidicon frame. While a start has been made on setting up such sequences in the northern hemisphere (Christian 1980), none of these could be observed from CTIO. Photoelectric standards are available in some clusters, but few are accurate below $V = 18$, and none are distributed in the sky in a way which would permit simultaneous observation with a 90 arcsec^2 field. As an alternative, it was decided that cluster fields which con-

tained a significant number of stars with photographic photometry calibrated with reliable photoelectric standards would be used to calibrate the vidicon data. Since the program fields in NGC 2204 contained stars with photographic photometry (Hawarden 1976), it was felt that these program stars could be used at least to define the zero points of the transformation equations between instrumental and BV colors and magnitudes for each field for each night, while suitable calibration fields, with a wider range in magnitude, would be used to define the slope of the transformation equations. Except for some crowded cluster fields in the Magellanic Clouds, the only photoelectrically calibrated photographic photometry for a cluster which contains stars with V greater than 19, accessible on nights when NGC 2204 is observed, and suitable for calibration of the 90 arcsec² vidicon frames is that of BDK for the cluster E3. A field close to the center of the latter cluster was chosen to maximize the number of stars and the magnitude range available for calibration.

Examination of the instrumental magnitudes of the different fields for each night for the two clusters showed that significant night-to-night shifts in the zero level of the instrumental magnitude scale were present in the data. These shifts were as large as several tenths of a magnitude and tended to be larger in B than in V . Although the nights were all dark and of photometric quality, it is difficult to attribute these shifts to causes other than changing atmospheric conditions, although some small contribution from changes in tube sensitivity cannot be ruled out. Also, no measurable shifts during any given night were found. The important point to make, though, is that these scale changes were found to be *completely independent of magnitude* (and hence of color, since nearly all of the stars measured lie along a well defined sequence in V , $[B - V]$), and thus it was a simple matter to place all of the data for a given field on the same instrumental system. This result emphasizes the value of having some means of internally normalizing the photometric zero point within a program field rather than relying on that obtained from another observation.

In the final calibration of photoelectric photometry, the major concerns are instrumental stability, color effects, and linearity.

a) Stability

Plotted in Figures 1a and 1b are the standard errors in a single observation as a function of the adjusted magnitude index for V and B , respectively, for the NGC 2204 fields (constants were added to the instrumental magnitudes to bring them close to the true BV system). The plots demonstrate that the vidicon system is capable of producing accurate photometry ($\sigma \lesssim 0.10$ mag) to $V \approx 21$ and $B \approx 21.5$ in a 45 minute exposure on a 1.5 m telescope. More importantly, for the fainter stars the errors are comparable to what one expects from photon statistics alone.

b) Color Terms

As with photographic and single star photoelectric photometry, care must be taken to ensure that the instrumental magnitudes and colors transform to the same system as the standard stars. The most significant of the secondary effects in such a transformation is that of the color terms in the transformation equation. While technically a vidicon is a photoelectric detector, the magnitude calibration is defined by the internal system of the standard stars within the frame, similar in principle to the case of a photographic plate with photoelectric standards. Since no fields other than those in E3 are used in the calibration, the derivation of the color term was accomplished using a technique identical to that for photographic work, with the assumption that the color effect is the same for all fields over the period of the run. The procedure is as follows. Given the photographic magnitudes of the stars in E3, a linear least squares solution was obtained for the correlation between V_{pg} and V' , and B_{pg} and B' , where V' and B' represent the averaged instrumental magnitudes. (The subscript pg as used in this paper refers to photographic in the

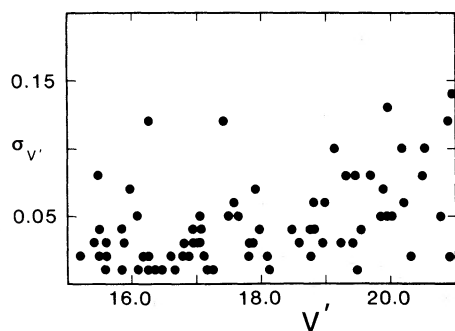


FIG. 1a

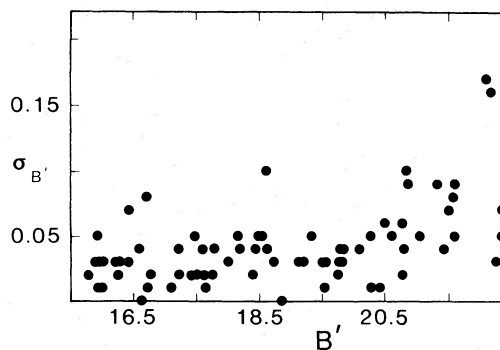


FIG. 1b

FIG. 1.—(a) Mean error for a single observation as a function of instrumental V magnitude in NGC 2204. (b) Same as Fig. 1a for instrumental B magnitudes.

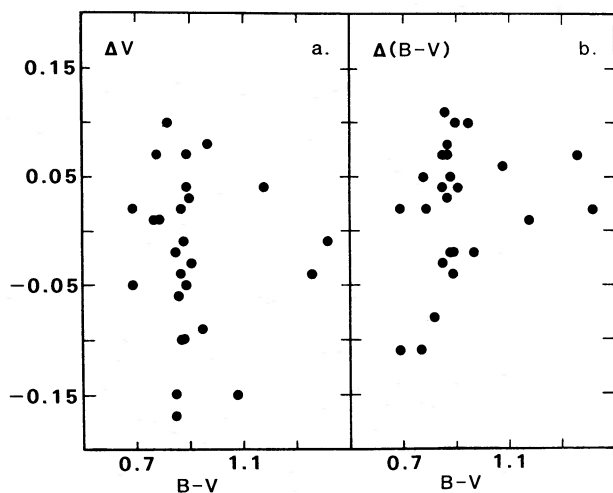


FIG. 2.—(a) Magnitude and (b) color residuals as a function of color from comparison of color-corrected photometry of van den Bergh, Demers, and Kunkel (1980) with transformed vidicon data.

sense that the standard star magnitudes are photographically derived and have been transformed to the photoelectric standard system of BDK.) The residuals, $(V' - V_{pg})$ and $(B' - B_{pg})$, were plotted versus $(B - V)_{pg}$ for a narrow magnitude range, approximately 3 mag, and the slope of the relation was taken as the color term. Using the photometry of BDK, the color equations were found to be

$$\begin{aligned} V_{pg}' &= V_{pg} - 0.05(\pm 0.10) * (B - V)_{pg} \\ B_{pg}' &= B_{pg} - 0.30(\pm 0.10) * (B - V)_{pg}, \end{aligned} \quad (1)$$

where V_{pg}' and B_{pg}' refer to the photographic magnitudes of BDK corrected for the color term. With the standards

corrected for color effects, the linear transformation between the instrumental and standard star systems was redetermined. The residuals, defined as $(V_{pg}' - V')$ and $(B_{pg}' - V_{pg}') - (B' - V')$, can be seen in Figures 2a and 2b, respectively, plotted versus $(B - V)_{pg}$.

c) Linearity

Since vidicon photometry in the equilibrium mode is similar to photoelectric photometry in terms of linearity, one should be able to extrapolate the calibration curve derived from the bright standards down to the limit of the instrument. The transformation curves derived after correction for color effects can be seen in Figures 3a and 3b for V' and B' , respectively, along with the observational data, and are found to be

$$\begin{aligned} V_{pg}' &= 0.986(\pm 0.014) * V' + 0.104 \\ B_{pg}' &= 1.013(\pm 0.017) * B' - 0.620, \end{aligned} \quad (2)$$

where the uncertainty represents the standard error in the estimate of the slope. The transformations show no indication of significant nonlinearity over the magnitude range available.

The vidicon instrumental magnitudes for NGC 2204 were transformed to the photoelectric system of BDK in E3 with the color equation and calibration curves of equations (1) and (2). The photometry is plotted in Figure 4 where superposed are the theoretical isochrones of Ciardullo and Demarque (1977) transformed to the observational plane (Ciardullo and Demarque 1979) for the composition $Y = 0.30$ and $Z = 0.007$, and ages 1, 2, 3, and 4×10^9 yr. This set of isochrones was chosen for consistency with published work on NGC 188, M67, NGC 2420, and NGC 2506, the other old disk clusters for which accurate photometry exists down to the unevolved main sequence (Demarque and McClure

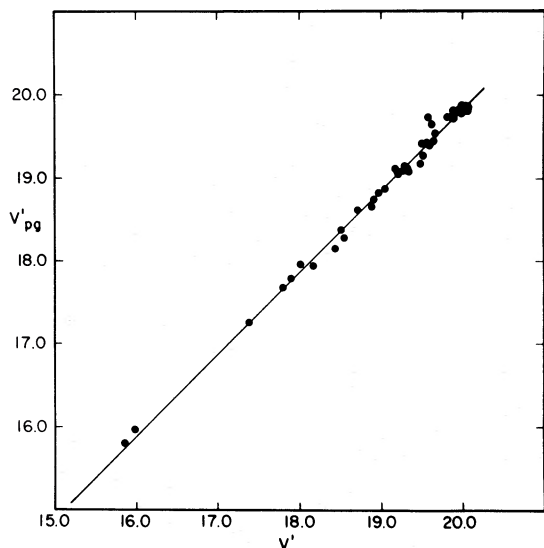


FIG. 3a

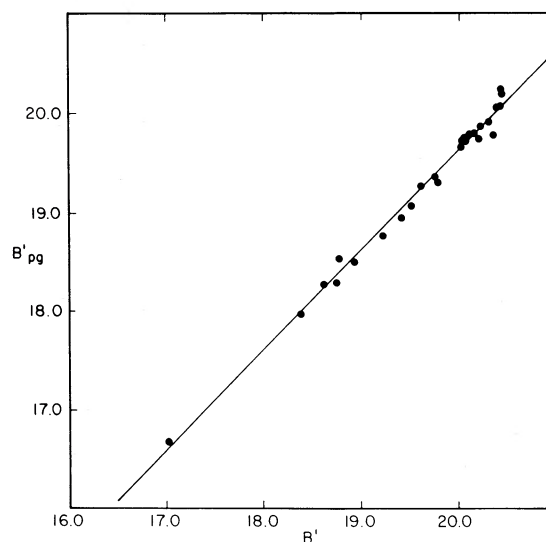


FIG. 3b

FIG. 3.—(a) Comparison of calibrated vidicon photometry in E3 with color-corrected photographic data of van den Bergh, Demers, and Kunkel (1980) for V . Solid line is linear relation of eq. (1). (b) Same as Fig. 3a for B magnitudes.

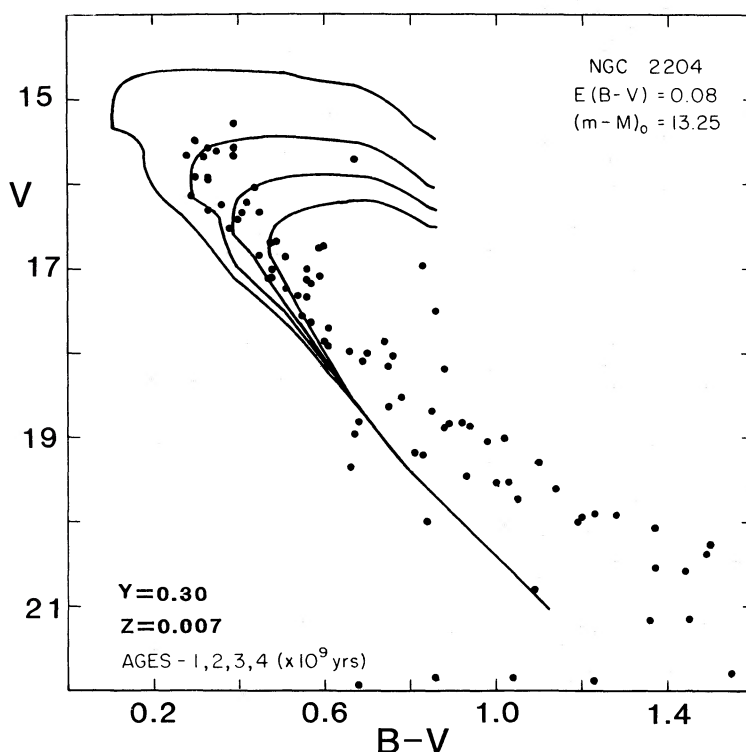


FIG. 4.—Color-magnitude diagram of vidicon photometry in NGC 2204 calibrated with photographic results of van den Bergh, Demers, and Kunkel (1980) in E3. Solid lines are isochrones of Ciadullo and Demarque (1977) for $Z = 0.007$, $Y = 0.30$, ages 1, 2, 3, and 4×10^9 years adjusted for $E(B-V) = 0.08$ and $(m-M) = 13.5$.

1977; Twarog 1978; McClure, Newell, and Barnes 1978; McClure, Twarog, and Forrester 1981). The metallicity is appropriate for NGC 2204 as determined from UBV photometry (Hawarden 1976) and DDO photometry (Dawson 1981). The isochrones have been adjusted for an assumed reddening of $E(B-V) = 0.08$ (Hawarden 1976) and an apparent distance modulus of $(m-M) = 13.50$. One point is immediately obvious. While the stars at the turnoff are consistent with the theoretical isochrone with an age of about 2×10^9 yr, as one goes to fainter magnitudes, the observed photometry deviates from the track by an increasing amount: The observed main sequence is significantly shallower than the theoretical main sequence. This cannot be the result of incorrect values for the reddening and the distance modulus. The three most likely causes for this discrepancy are the following:

1. *The isochrones are incorrect.*—Comparison of the same theoretical models to the cluster data for NGC 2420 (McClure, Newell, and Barnes 1978) and NGC 2506 (McClure, Twarog, and Forrester 1981), slightly older clusters of similar metallicity, shows no significant discrepancy to a $(B-V)$ equivalent to 0.8 in Figure 4. Comparison of more metal-rich clusters such as the Hyades allows a check of the lower main sequence for more metal-rich models. B. Anthony-Twarog (1981, private communication) finds good agreement to $(B-V)_0 \approx 1.0$. Beyond this point, the observed data have a shallower slope, but the effect is far smaller than

that of Figure 4. Finally, the slope of the faint ZAMS based on nearby field stars (Woolley *et al.* 1970), the Hyades, and M67 (Racine 1971) is found to be the same, approximately 5, while the data for NGC 2204 give a slope of 3. Though the mean metallicity of the field stars and clusters is higher than that of NGC 2204, the effect on the slope of the main sequence should be negligible.

2. *The E3 calibration does not apply to NGC 2204.*—One might argue that the vidicon system changes over a night of observation, and therefore the calibration derived from fields obtained in the latter half of the night at a particular hour angle may not be valid for a second field taken earlier at a different hour angle. In particular, a calibration difference might arise from the simple annular reduction procedure if the image profile for the stars is significantly altered at higher air mass. We regard this as unlikely because, as will be shown below, the problem seems to be a magnitude dependent one occurring primarily in the B filter. More importantly, the results of Figure 3 show that with only a zero point correction for each field, the internal accuracy of the instrumental magnitudes when four nights of observation are compared is quite high, so that significant changes in the slope of the calibration can be excluded.

3. *There is a systematic error in the calibration standards.*—Such an error could arise in two ways: (a) The photoelectric standards of BDK could be in

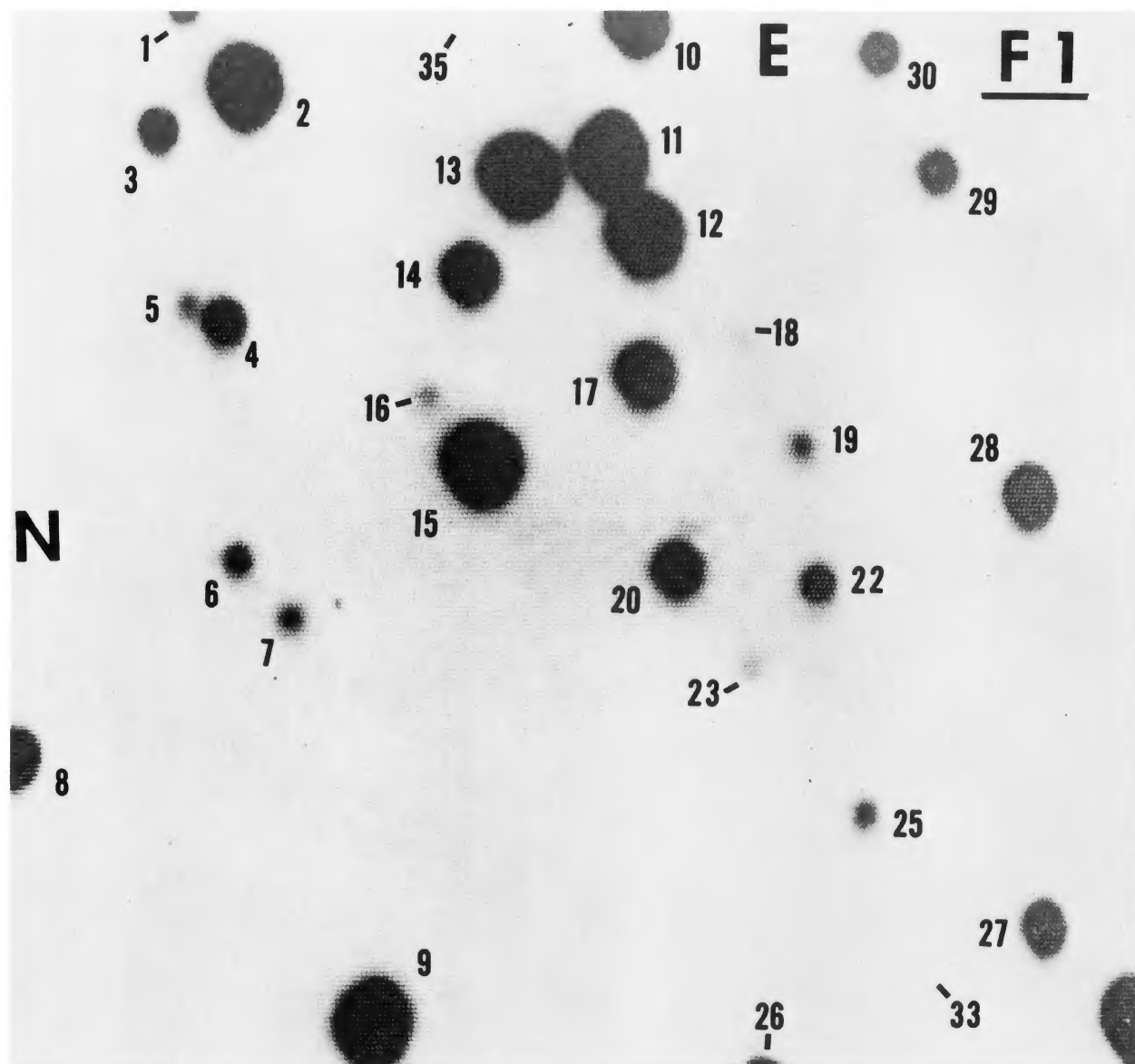


FIG. 5a

FIG. 5.—Identification charts for stars in the three fields of NGC 2204. They are about 90" on a side.

error; or (b) The photographic photometry of BDK has been incorrectly transformed to the system of the photoelectric standards. Since only two of the brighter photoelectric standards are within the calibration field of the vidicon and the remainder of the E3 standards for the present reduction have only photographically derived magnitudes, there is no direct way to distinguish between the two possibilities. To test for possible systematic differences between the fields of NGC 2204 and E3, the color terms and transformation curves for the instrumental system were redetermined using the photographic photometry of Hawarden (1976) within NGC 2204 alone. While the number of stars, the color range, and the magnitude range were smaller than for E3, the results proved to be of comparable accuracy. It was determined that the color terms were consistent

with those in equation (1), while the linear transformations were

$$\begin{aligned} V_{pg}' &= 0.963(\pm 0.017) * V' + 0.60 \\ B_{pg}' &= 0.936(\pm 0.017) * B' + 0.94. \end{aligned} \quad (3)$$

Only stars with V brighter than 17.0 were included in the calibration. Comparison of equations (2) and (3) demonstrate that while the slope of the V' transformation is the same within the uncertainties for the two clusters, the B' slope is significantly smaller for NGC 2204 than for E3.

If this difference is real, what is its cause, and how can it be determined? While we feel that the slope of the transformation curve for NGC 2204 is correct and that of E3 is in error because of a probable systematic

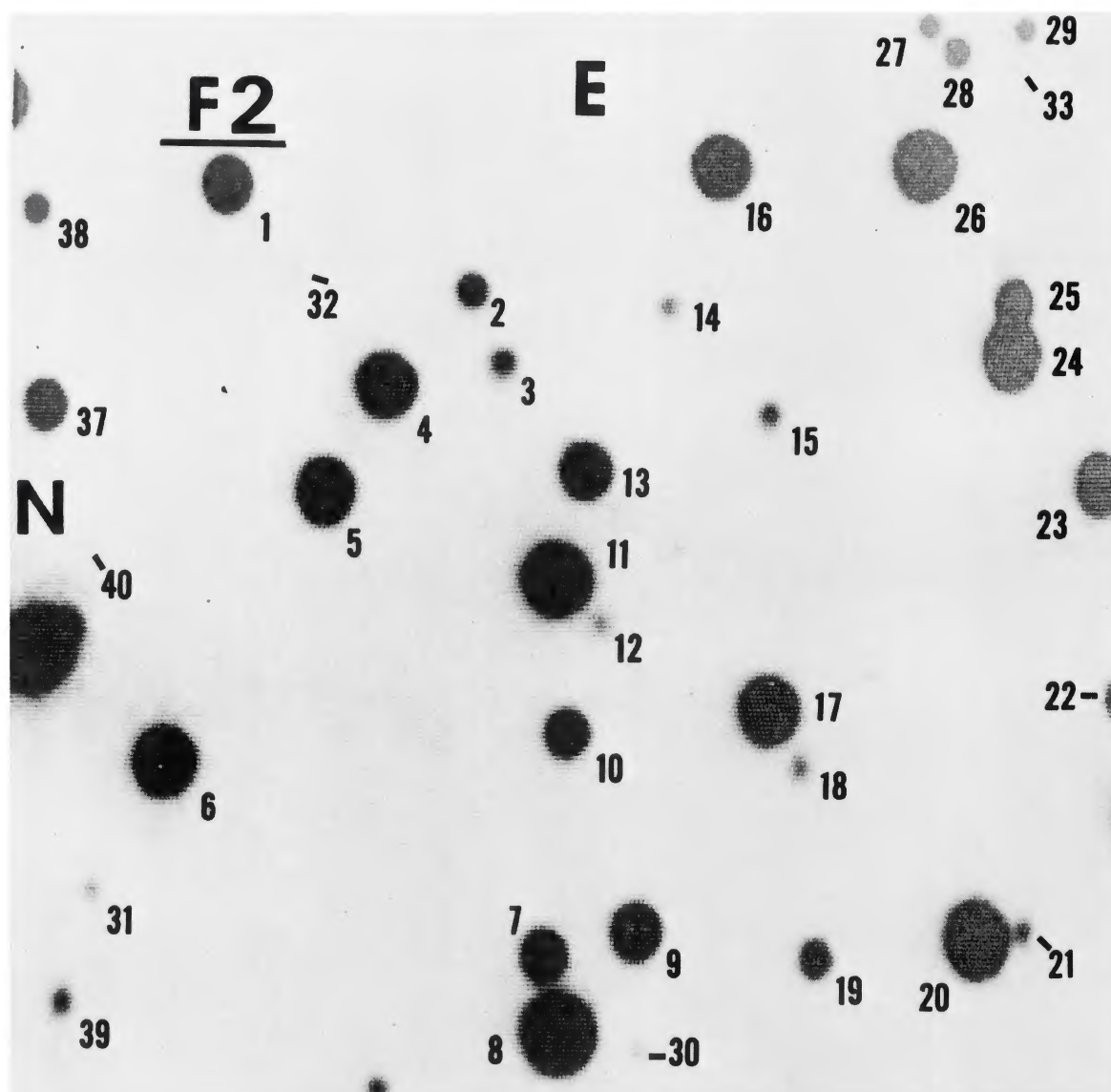


FIG. 5b

error in the B photometry of BDK, we also recognize that this can be verified only by direct photoelectric photometry within E3. Short of this, one is left with inference based upon a choice of which transformation provides a $C-M$ diagram that compares more favorably to available $C-M$ diagrams of analogous clusters. Such a comparison will be the topic of § IV.

IV. THE COLOR-MAGNITUDE DIAGRAMS

a) NGC 2204

Once again, the instrumental magnitudes for the stars in the fields of NGC 2204 were transformed to the photoelectric system using the calibration curves of equation (3) and the color terms of equation (1). The stars are identified in Figure 5, and the final magnitudes and the mean error for a single observation are listed in Table 1, along with the number of observations in

each color. The stars for which crowding forced the use of a diaphragm of radius 3 pixels rather than 6 are indicated with a footnote. The $C-M$ diagram is plotted in Figure 6. Superposed are the theoretical isochrones described in § III, adjusted for a reddening of $E(B-V) = 0.08$ (Hawarden 1976), but an apparent distance modulus of $(m-M) = 13.40$. Since the reddening is determined independent of the present data or isochrone fit, the fit itself, and the distance modulus, can be obtained only by vertical shifts between the isochrones and the data. The important features to be noted are the following:

1. The unevolved main sequence compares quite well with the theoretical models down to about $(B-V) = 0.9$ and $V = 20.0$. Beyond these values, the data become dominated by uncertainties in the photometry.

2. The photometry of the brighter end contains somewhat more scatter than one might expect on the basis

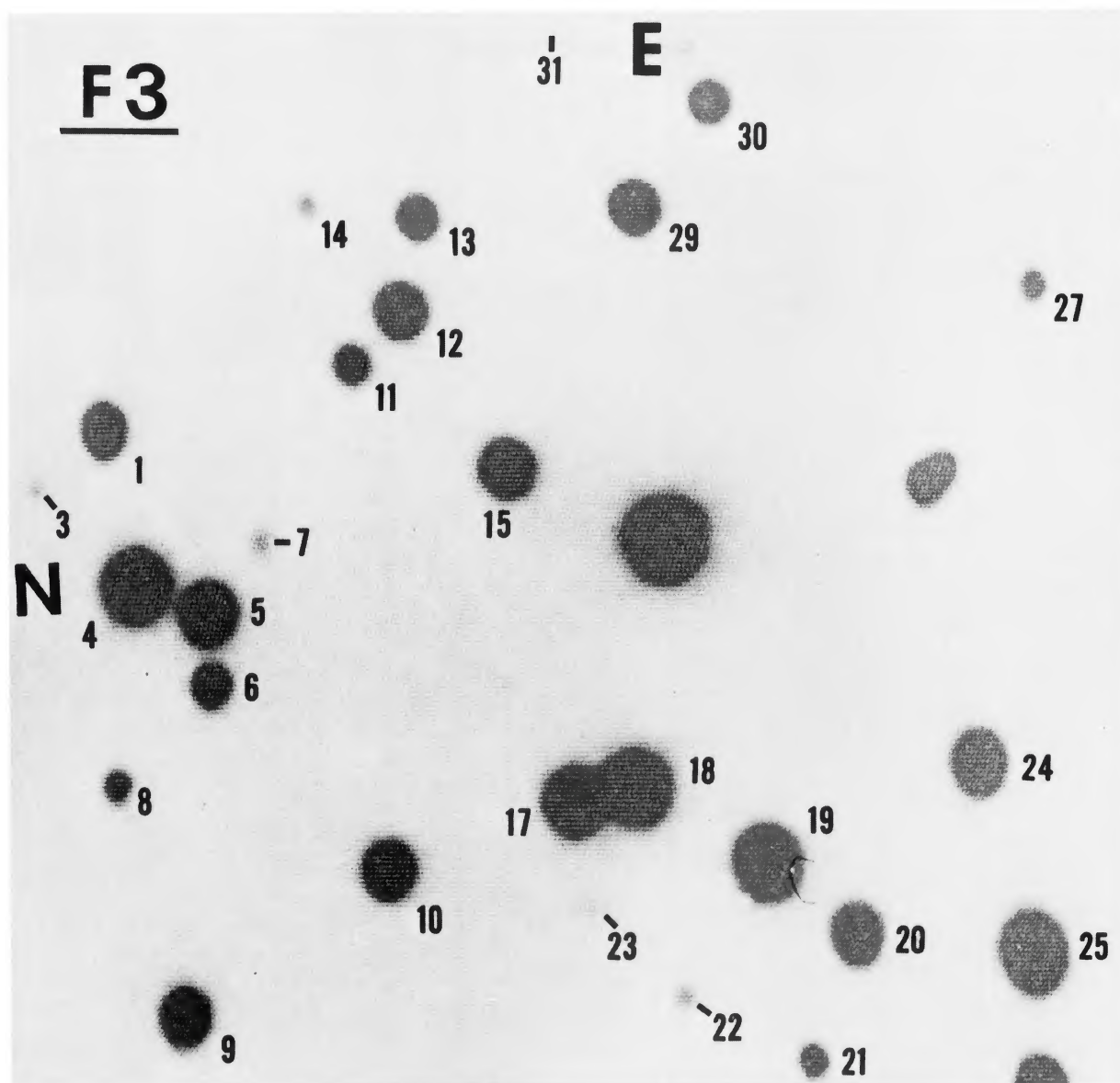


FIG. 5c

of the internal scatter in the instrumental magnitudes. One possible explanation is that there is a significant number of binary systems, concentrated near the center of the cluster because of their higher mass. However, Twarog (1983) has found a similar effect in the old cluster NGC 752 with the same age as NGC 2204 and has shown that the scatter is bimodal and not the result of binaries. The most plausible explanation in the NGC 752 case appears to be rotation. The scatter below the main sequence for $V \approx 18.5$ is probably due to field star contamination. Though the fields were chosen to be within the central regions of the cluster to maximize the observation of cluster members, below $V = 19$ the contribution from background stars will become non-negligible in this area of the Galaxy. Table 5 of Bahcall and Soneira (1980) predicts that we should see 10–20

stars in the range $18.5 \leq m_v \leq 20.5$ in the SIT fields which cover NGC 2204.

3. The apparent color of the turnoff is found to be $(B - V) = 0.37 \pm 0.02$, which is consistent with an age of $2.5 \pm 0.3 \times 10^9$ yr. Assuming that $A_v = 3.3 \times E(B - V)$, the true distance modulus of the cluster is $(m - M)_0 = 13.13 \pm 0.20$, implying that the cluster is 1170 pc above the Galactic plane.

4. Hawarden (1976) observed that the red giant clump in NGC 2204 was at $V = 13.82$. Combined with the apparent distance modulus of 13.40, this leads to $M_v = +0.4$ (+0.5 if stars with uncertain photometry in Hawarden 1976 are discarded) for these post-helium core flash stars. From the same isochrones, McClure, Twarog, and Forrester (1981) derive $M_v = +0.8$ for both NGC 2420 and NGC 2506. The brighter intrinsic

luminosity for the clump stars in NGC 2204 is somewhat unexpected given the fact that NGC 2204 is younger than either NGC 2420 or NGC 2506 by only 10^9 yr.

The final feature to be discussed for NGC 2204 is the luminosity function. The number of stars as a function of B magnitude for B greater than 15 were counted, and the resulting distribution can be seen in Figure 7 (solid line). B magnitudes were used so that a direct comparison could be made with the work of Chiu and van Altena (1981) on NGC 2506. The brightest and faintest bins are not well determined because of magnitude limitations on the program stars.

Figure 7 demonstrates that the luminosity function is strongly peaked over the first 2 mag below the turnoff, remains effectively flat for 3 mag, and may decline sharply below $B = 21$ ($M_v \simeq 6.5$). Since membership probabilities are unavailable for any of these stars, one might wonder to what degree the luminosity function is affected by field star contamination. Estimates of the number of field stars as a function of B magnitude were obtained by combining the total area of the three program fields and the differential star densities of Bahcall and Soneira (1980) for $l = 180^\circ$ and $b = 20^\circ$. While NGC 2204 is at slightly lower Galactic latitude, the error in the field counts should be minor except for the last two luminosity bins and will serve only to enhance the effects described above. The corrected luminosity function is given by the dashed line in Figure 7. As mentioned earlier, the peak near the turnoff may

TABLE 1
VIDICON PHOTOMETRY IN NGC 2204

Field-No.	Hawarden No.	V	N_V	B	N_B
1-1	...	18.85 ± 0.08	2	$19.32 \pm \dots$	1
1-2	...	15.59 ± 0.03	3	16.00 ± 0.01	3
1-3	...	18.00 ± 0.03	3	18.55 ± 0.04	3
1-4 ^a	...	17.90 ± 0.02	2	18.47 ± 0.05	3
1-5 ^a	...	19.77 ± 0.02	3	20.74 ± 0.10	3
1-6	...	19.08 ± 0.05	3	19.68 ± 0.03	3
1-7	...	19.39 ± 0.04	3	20.15 ± 0.01	3
1-8	...	17.26 ± 0.03	2	$17.74 \dots$	1
1-9	1211	15.68 ± 0.03	3	16.38 ± 0.03	3
1-10	1142	16.63 ± 0.00	2	17.08 ± 0.01	2
1-11 ^a	1146	16.01 ± 0.07	3	16.47 ± 0.07	3
1-12 ^a	1143	15.89 ± 0.04	3	16.23 ± 0.03	3
1-13 ^a	1144	15.53 ± 0.08	3	15.97 ± 0.03	3
1-14	1145	17.11 ± 0.02	3	17.61 ± 0.02	3
1-15	1147	15.65 ± 0.03	3	16.09 ± 0.03	3
1-16 ^a	...	19.93 ± 0.05	3	20.97 ± 0.05	3
1-17	1148	16.95 ± 0.03	3	17.38 ± 0.02	3
1-18 ^a	...	20.98 ± 0.20	3	22.02 ± 0.16	3
1-19	...	19.40 ± 0.01	3	20.14 ± 0.05	3
1-20	1149	17.62 ± 0.05	3	18.12 ± 0.04	3
1-22	...	18.69 ± 0.04	3	19.18 ± 0.05	3
1-23	...	20.38 ± 0.08	3	21.39 ± 0.07	3
1-25	...	19.17 ± 0.03	3	20.02 ± 0.04	3
1-26 ^a	...	$16.70 \dots$	1	$17.25 \dots$	1
1-27	1116	17.42 ± 0.12	2	18.17 ± 0.05	3
1-28	1118	17.07 ± 0.04	3	17.57 ± 0.04	3
1-29	...	18.09 ± 0.01	3	18.81 ± 0.00	3
1-30	...	18.06 ± 0.02	3	18.66 ± 0.03	3
1-33	...	20.94 ± 0.17	3	22.16 ± 0.06	2

TABLE 1—Continued

Field No.	Hawarden No.	V	N_V	B	N_B
1-35 ^a	...	21.01 ± 0.02	2	22.24 ± 0.07	2
2-1	3116	16.81 ± 0.03	3	17.28 ± 0.03	3
2-2	...	18.71 ± 0.02	3	19.40 ± 0.03	3
2-3	...	19.33 ± 0.03	3	20.01 ± 0.05	3
2-4	3117	16.47 ± 0.01	3	16.84 ± 0.01	3
2-5	3118	16.61 ± 0.02	3	17.08 ± 0.02	3
2-6	3121	16.19 ± 0.02	3	16.56 ± 0.01	3
2-7 ^a	3128	17.55 ± 0.06	3	18.02 ± 0.04	3
2-8	3129	15.28 ± 0.02	3	15.75 ± 0.03	3
2-9	3127	17.02 ± 0.03	3	17.55 ± 0.03	3
2-10	3124	17.78 ± 0.03	3	18.27 ± 0.03	3
2-11	3123	15.89 ± 0.01	3	16.26 ± 0.03	3
2-12	...	20.63 ± 0.05	3	21.36 ± 0.08	3
2-13 ^a	3122	17.15 ± 0.01	3	17.60 ± 0.01	3
2-14	...	19.76 ± 0.05	3	20.68 ± 0.04	3
2-15	...	19.46 ± 0.04	3	20.32 ± 0.01	3
2-16	3208	16.29 ± 0.02	3	16.74 ± 0.01	3
2-17	3125	16.27 ± 0.01	3	16.61 ± 0.00	3
2-18 ^a	...	19.41 ± 0.08	3	20.82 ± 0.06	3
2-19	...	18.55 ± 0.03	3	19.10 ± 0.03	3
2-20	3126	15.66 ± 0.02	3	16.04 ± 0.01	3
2-21 ^a	...	19.84 ± 0.13	3	20.04 ± 0.05	3
2-22	...	$18.57 \dots$	1	$19.23 \dots$	1
2-23 ^a	3211	16.68 ± 0.01	3	17.24 ± 0.04	3
2-24	3210	16.18 ± 0.01	3	16.61 ± 0.04	3
2-25 ^a	...	17.88 ± 0.07	3	18.41 ± 0.05	3
2-26	3209	15.92 ± 0.03	3	16.29 ± 0.02	3
2-27 ^a	...	19.22 ± 0.08	2	19.65 ± 0.04	2
2-28	...	18.76 ± 0.04	3	19.43 ± 0.01	3
2-29 ^a	...	19.06 ± 0.10	3	19.65 ± 0.04	3
2-30 ^a	...	20.42 ± 0.10	3	21.49 ± 0.05	3
2-31	...	20.22 ± 0.02	3	21.35 ± 0.04	3
2-32	...	20.95 ± 0.14	3	22.26 ± 0.05	3
2-33 ^a	...	20.78 ± 0.12	3	22.11 ± 0.16	3
2-37 ^a	...	17.47 ± 0.05	2	17.93 ± 0.03	2
2-38 ^a	...	18.75 ± 0.06	2	19.47 ± 0.02	2
2-39	...	19.59 ± 0.08	2	20.36 ± 0.06	2
2-40 ^a	...	20.79 ± 0.02	3	22.00 ± 0.16	3
3-1	...	17.24 ± 0.01	3	17.71 ± 0.02	3
3-3	...	20.10 ± 0.10	3	21.62 ± 0.09	3
3-4	...	15.55 ± 0.02	3	15.99 ± 0.05	3
3-5 ^a	2123	16.29 ± 0.12	3	16.71 ± 0.08	3
3-6 ^a	...	17.94 ± 0.04	3	18.56 ± 0.10	3
3-7	...	20.10 ± 0.06	3	21.25 ± 0.09	3
3-8	...	18.88 ± 0.03	3	19.67 ± 0.02	3
3-9	2107	17.04 ± 0.05	3	17.45 ± 0.02	3
3-10	2108	16.94 ± 0.04	4	17.44 ± 0.05	4
3-11	...	18.42 ± 0.04	4	19.02 ± 0.03	4
3-12	2112	17.04 ± 0.03	4	17.47 ± 0.02	4
3-13	...	17.83 ± 0.03	4	18.31 ± 0.02	4
3-14	...	19.79 ± 0.07	4	20.69 ± 0.04	4
3-15	2111	16.78 ± 0.02	4	17.19 ± 0.02	4
3-17 ^a	...	16.11 ± 0.05	4	16.42 ± 0.03	4
3-18 ^a	2110	15.55 ± 0.04	4	15.94 ± 0.03	4
3-19	3104	15.63 ± 0.01	4	15.97 ± 0.03	4
3-20	3105	16.78 ± 0.02	4	17.19 ± 0.02	4
3-21 ^a	...	18.71 ± 0.02	4	19.42 ± 0.03	4
3-22	...	19.86 ± 0.05	4	20.74 ± 0.09	4
3-23	...	20.98 ± 0.08	4	21.93 ± 0.17	4
3-24	3108	16.37 ± 0.01	4	16.77 ± 0.02	4
3-25	3107	15.47 ± 0.03	4	15.84 ± 0.02	4
3-27	...	18.92 ± 0.06	4	19.67 ± 0.03	4
3-29	3110	16.90 ± 0.02	4	17.66 ± 0.02	4
3-30	...	17.78 ± 0.02	4	18.39 ± 0.04	4
3-31	...	20.85 ± 0.14	4	22.27 ± 0.14	4

^a Smaller diaphragm used in photometry.

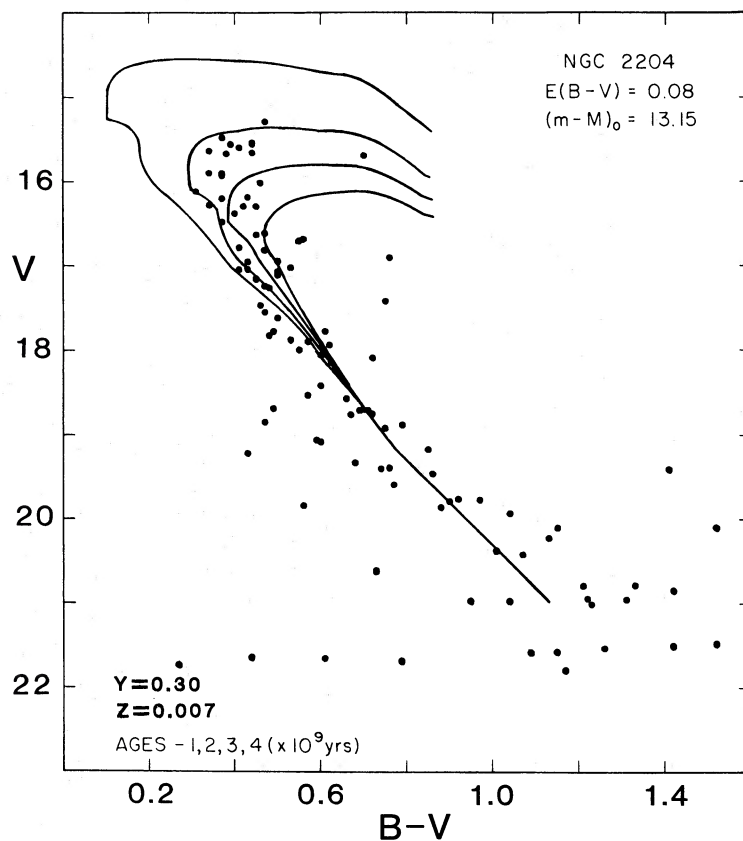


FIG. 6.—Color-magnitude diagram of vidicon photometry in NGC 2204 calibrated with photographic results of Hawarden (1976) in NGC 2204. Solid lines are same as in Fig. 4 with $(m-M) = 13.4$.

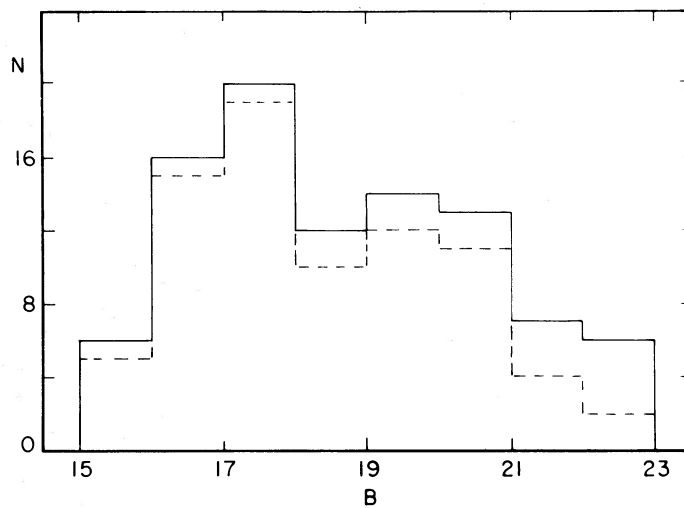


FIG. 7.—Luminosity function for NGC 2204 (solid line). Luminosity function corrected for probable field star contamination based on work of Bahcall and Soneira (1980) (dashed line).

be the product of mass segregation acting on the higher mass binaries. The constancy of the mass function between $B = 18$ and 21 is in agreement with the results of McClure, Forrester, and Gibson (1974) for NGC 2420 but contrasts strongly with the data on NGC 2506, where Chiu and van Altena (1981) find a significant drop in the luminosity function below $M_v \simeq 4$ ($B \simeq 18$ for NGC 2204). Chiu and van Altena offer three possible explanations for the differences between the luminosity functions of NGC 2506 and NGC 2420: (a) The initial mass function varies from cluster to cluster; (b) Stripping of low mass stars is more frequent for NGC 2506 which lies only 480 pc away from the Galactic plane compared to 750 pc for NGC 2420; and (c) The total mass of NGC 2506 is less than that of NGC 2420, leading to an increased rate of evaporation for NGC 2506. Note that the lack of a turnover in the luminosity function down to $B = 21$ for NGC 2204 is consistent with explanation (b) above in that NGC 2204 is both younger and located further from the Galactic plane than either NGC 2506 or NGC 2420. Mass segregation effects, if present, will cause lower mass, fainter stars to be found preferentially in the outer, unstudied region of the cluster. Hence, inclusion of these

effects would tend to decrease the slope of the luminosity function even further.

b) E3

The vidicon data for E3 were analyzed with the assumption that the calibration based on the standards in NGC 2204 was correct rather than that based on the photometry of BDK. The vidicon magnitudes were transformed to the photoelectric system using the calibrations of (3) and the color terms of equation (1). The zero points for the transformations were determined from the BDK values for stars K and L, the only two photoelectric standards in the program field of E3. The transformed vidicon photometry is listed in Table 2, along with the appropriate BDK number for stars in common, the mean errors for a single observation in each color, and the number of observations for each star, while the resultant $C-M$ diagram is shown in Figure 8. The scatter in the photometry is larger than for NGC 2204 because of shorter total integration times for each E3 frame. The identification chart for stars in the present study can be found in Figure 9.

The entire photographic sample of BDK can be transformed to the BV system as defined by the vidicon

TABLE 2
VIDICON PHOTOMETRY IN E3

FT No.	BDK No.	V	N_V	B	N_B	FT No.	BDK No.	V	N_V	B	N_B
1	153	18.80 ± 0.09	3	19.84 ± 0.04	2	38	103	18.77 ± 0.03	3	19.49 ± 0.04	2
2	134	20.39 ± 0.06	3	20.93 ± 0.04	2	39	139	18.44 ± 0.05	3	19.27 ± 0.07	2
3	154	20.24 ± 0.07	3	20.89 ± 0.12	2	40	55	19.03 ± 0.07	3	19.75 ± 0.11	2
4	114	$19.47 \dots$	1	$20.20 \dots$	1	41	61	19.34 ± 0.06	3	20.03 ± 0.07	2
5	155	18.90 ± 0.02	3	19.39 ± 0.04	2	42	40	17.90 ± 0.04	2	$18.50 \dots$	1
6	135	19.87 ± 0.09	3	20.46 ± 0.01	2	43	73	19.85 ± 0.03	3	20.57 ± 0.08	2
7	136	17.71 ± 0.01	3	18.37 ± 0.03	2	44	72	19.06 ± 0.04	2	$19.67 \dots$	1
8	137	19.19 ± 0.01	3	19.81 ± 0.08	2	45	74	19.80 ± 0.03	3	20.38 ± 0.02	2
9	138	19.72 ± 0.02	3	20.39 ± 0.06	2	46	80	19.49 ± 0.02	3	20.04 ± 0.01	2
10	156	18.06 ± 0.03	3	18.66 ± 0.01	2	47	L	15.97 ± 0.03	3	16.98 ± 0.03	2
11	171	17.32 ± 0.04	3	18.24 ± 0.03	2	48	K	15.86 ± 0.02	3	17.04 ± 0.01	2
12	157	19.14 ± 0.06	3	19.87 ± 0.07	2	49	172	19.81 ± 0.03	3	20.53 ± 0.04	2
13	173	18.39 ± 0.01	3	19.11 ± 0.05	2	50	...	18.28 ± 0.06	3	19.11 ± 0.05	2
14	158	17.80 ± 0.02	3	18.51 ± 0.08	2	51	...	20.53 ± 0.01	3	21.26 ± 0.14	2
15	119	18.31 ± 0.01	3	18.94 ± 0.07	2	52	...	20.60 ± 0.13	2	$21.45 \dots$	1
17	120	19.64 ± 0.05	3	20.33 ± 0.07	2	53	...	20.45 ± 0.07	3	21.18 ± 0.07	2
18	107	18.59 ± 0.02	3	19.33 ± 0.08	2	54	...	19.18 ± 0.01	3	19.96 ± 0.01	2
19	108	19.79 ± 0.08	3	20.50 ± 0.04	2	55	...	20.91 ± 0.16	3	21.34 ± 0.06	2
20	106	19.40 ± 0.02	3	20.05 ± 0.01	2	56	...	20.80 ± 0.10	3	21.68 ± 0.15	2
21	121	19.46 ± 0.07	3	20.01 ± 0.05	2	57	...	20.65 ± 0.06	3	21.34 ± 0.01	2
22	84	19.97 ± 0.11	3	20.65 ± 0.25	2	58	...	20.64 ± 0.10	3	21.30 ± 0.01	2
23	76	$19.17 \dots$	1	$19.68 \dots$	1	60	...	20.19 ± 0.14	3	21.02 ± 0.17	2
24	75	18.86 ± 0.03	3	20.03 ± 0.05	2	62	...	20.11 ± 0.05	3	20.87 ± 0.23	2
25	83	20.13 ± 0.06	3	21.10 ± 0.03	2	64	...	19.76 ± 0.02	3	20.39 ± 0.01	2
26	96	19.05 ± 0.02	3	19.69 ± 0.04	2	66	...	20.75 ± 0.14	3	21.40 ± 0.04	2
27	82	20.25 ± 0.01	3	20.74 ± 0.01	2	67	...	20.11 ± 0.06	3	21.74 ± 0.14	2
28	81	19.43 ± 0.01	3	20.05 ± 0.04	2	68	...	19.74 ± 0.06	3	20.48 ± 0.01	2
29	95	19.36 ± 0.06	3	19.91 ± 0.01	2	69	...	20.83 ± 0.11	3	21.50 ± 0.14	2
30	94	20.36 ± 0.04	3	21.01 ± 0.21	2	70	...	20.82 ± 0.06	3	21.96 ± 0.06	2
31	93	19.14 ± 0.06	3	19.76 ± 0.06	2	71	...	18.44 ± 0.04	3	19.35 ± 0.04	2
32	92	19.70 ± 0.05	3	20.36 ± 0.06	2	73	...	20.85 ± 0.09	3	21.24 ± 0.04	2
33	117	19.42 ± 0.02	3	20.06 ± 0.01	2	74	...	21.16 ± 0.18	3	22.14 ± 0.21	2
34	116	19.87 ± 0.04	3	20.60 ± 0.15	2	75	...	20.88 ± 0.13	3	21.55 ± 0.14	2
35	115	19.73 ± 0.10	3	20.58 ± 0.06	2	77	...	21.06 ± 0.09	3	21.48 ± 0.20	2
36	104	19.33 ± 0.06	3	19.99 ± 0.10	2	78	...	19.58 ± 0.05	3	20.16 ± 0.02	2
37	105	20.27 ± 0.08	3	20.91 ± 0.01	2						

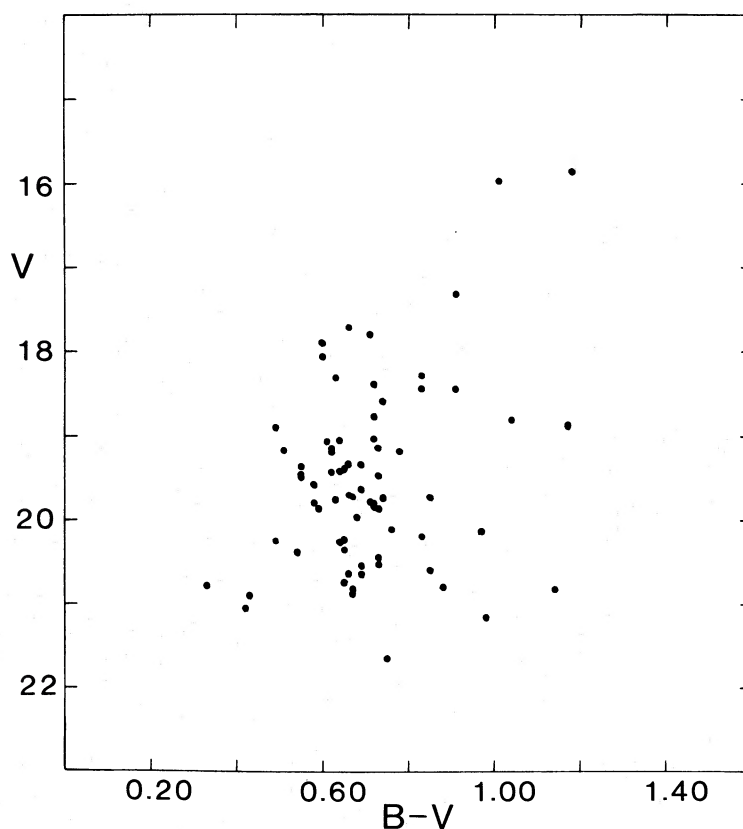


FIG. 8.—Color-magnitude diagram of vidicon photometry in E3 calibrated with photographic results of Hawarden (1976) in NGC 2204

calibrations of NGC 2204. Using the 46 stars common to both samples and the techniques described in § III, color terms and a linear transformation between the photographic photometry of BDK and the vidicon system were derived. (An additional star, FT 33, was not included in the transformation because of excessively large residuals. If the photometry of BDK is used, the star lies in an anomalous position in the $C-M$ diagram, while the vidicon data place the star at the cluster turnoff. Possible variability should be checked.) The use of a linear transformation is justified since the results of Figure 3 demonstrate that the photographic photometry of BDK is linearly related to the instrumental magnitudes of the vidicon, indicating that if an error exists in the photographic photometry of BDK, it affects primarily the slope of the photometry and not the linearity. No color term of significance was found, though the scatter in the residuals is large enough that a small term can be hidden. The derived transformations were

$$\begin{aligned} V_{pe} &= 0.980(\pm 0.013) * V_{BDK} + 0.359 \\ B_{pe} &= 0.894(\pm 0.011) * B_{BDK} + 1.874. \end{aligned} \quad (4)$$

The proximity of the V slope to 1.0 reemphasizes an earlier statement that the V magnitudes of BDK are quite compatible with those of the vidicon system and that the error probably lies in the B magnitude system.

The photographic data of BDK, transformed with the above calibrations and combined with the data of Table 2, are plotted in Figure 10. Stars common to the two samples were simply averaged; these stars are denoted in Figure 10 by crosses. Comparison of Figure 5 of BDK to Figure 10 reveals a number of differences:

1. The apparent scatter which exists in the $C-M$ diagram of BDK for stars brighter than $V = 17.5$ and bluer than the giant branch is present, but to a lesser degree. A significant fraction of the stars have shifted position in the $C-M$ diagram to produce an almost vertical giant branch at $(B-V) \sim 0.90$. The reality of this feature is confirmed in Figure 11 where only the stars within the core of the cluster as defined by BDK, $R \leq 1'2$, have been plotted. Superposed on the data is the normal sequence for the sparsely populated globular cluster, Pal 12, as determined from the photometry of Harris and Canerna (1980). The normal sequence has been aligned by matching the turnoff and the subgiant branch for the two clusters.

2. The color of the turnoff is approximately 0.2 mag bluer than that derived by BDK. This is not unexpected because the zero points of the transformations were derived using only two photoelectric standards, stars L and K, which may be in error. It had been hoped that a reasonable estimate of the correct color for the turnoff could be obtained from the morphology of the subgiant branch. For clusters of a given age, the more

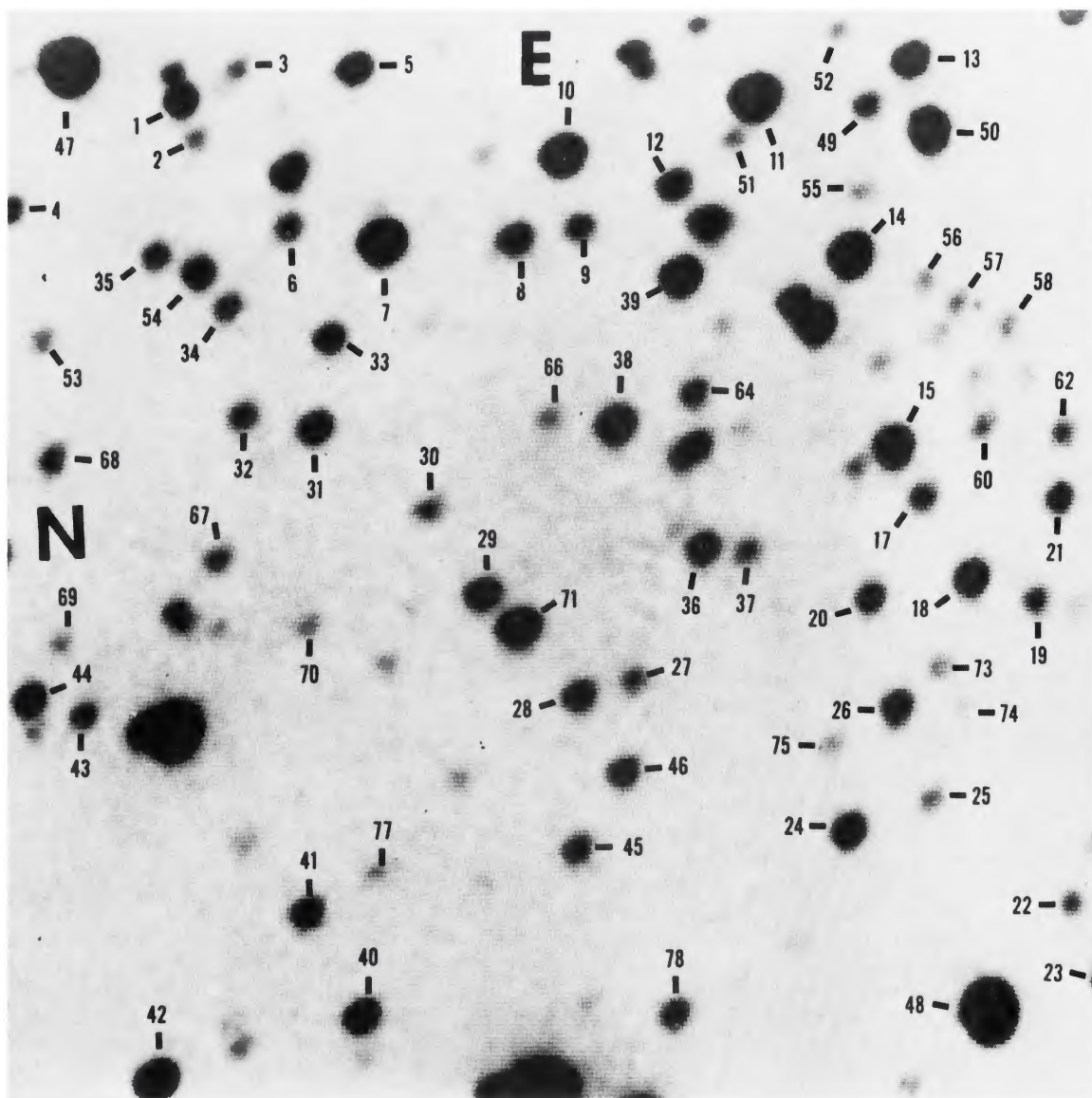


FIG. 9.—Identification chart for stars in E3. It is about 90" on a side.

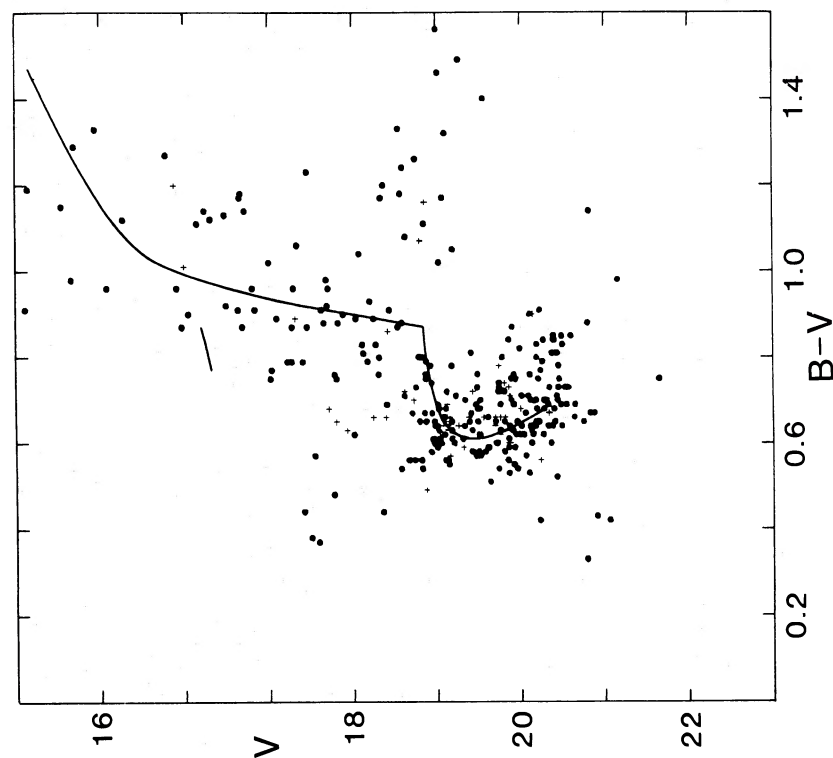


FIG. 10

FIG. 10.—Color-magnitude diagram of photographic photometry of van den Bergh, Demers, and Kunkel (1980) transformed to the vidicon system of NGC 2204. Solid line represents normal sequence of Pal 12 (Harris and Canterna 1980) aligned at the turnoff and subgiant branch.

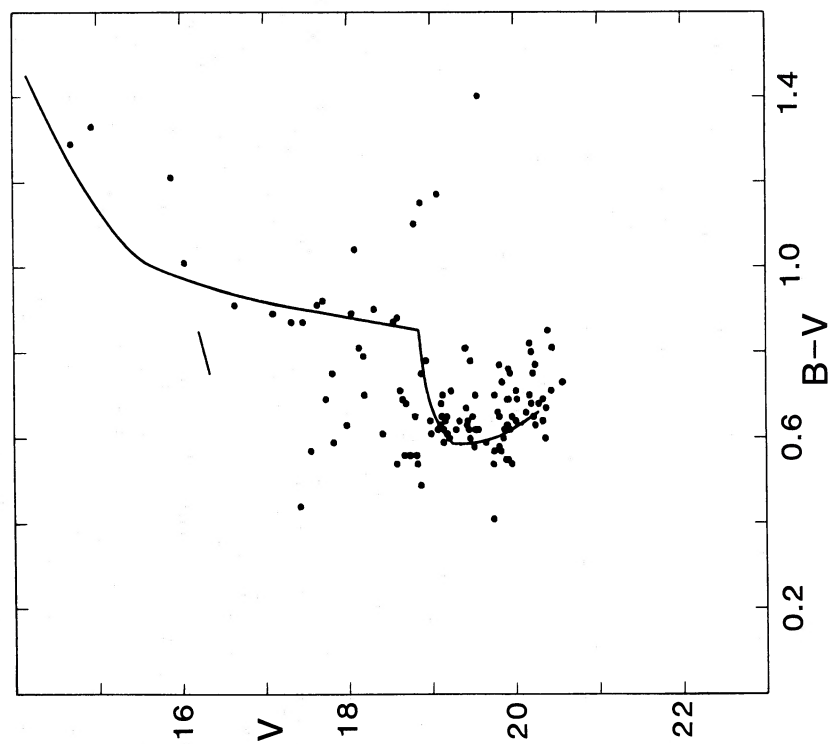


FIG. 11

FIG. 11.—Same as Fig. 10 for inner 1/2 of cluster

metal-rich clusters have shallower slopes on the subgiant branch. Since the width of the subgiant branch of E3 is consistent with an age similar to that of other globulars and the cluster reddening is known to ± 0.05 mag, knowledge of the cluster metallicity will permit an estimate of the true color of the cluster turnoff. Unfortunately, the sparse population of the cluster and the photometric uncertainty near the subgiant branch combined to make a distinction between even M92 and Pal 12 impossible.

3. Though the scatter is large, the ridge line for the stars at the turnoff in E3 is consistent with the main-sequence turnoffs of both Pal 12 and M92, in contrast with the data of BDK which show a sharp deviation to the red as V increases which cannot easily be matched by any existing cluster $C-M$ diagram.

4. Though some of the scatter above $V = 17.5$ has been removed in the present $C-M$ diagram, it should not be concluded that all the scatter blueward of the giant branch is artificial or due to field star contamination. Our photometry confirms the claim of BDK that E3 does have a population of anomalous stars which, under normal circumstances in an open cluster, would be classed as possible blue stragglers. Within a radius of $R = 2.4$, there are approximately 45 stars between $V = 16.9$ and 18.9 with $(B-V)$ less than 0.85 . Of these 45, 22 are found within $R = 1.2$, while the expected number for a random field star distribution is only 11. The concentration to the cluster core is especially easy to detect for the group of stars just brighter than and bluer than the cluster turnoff, the classic location for blue stragglers. If blue stragglers are binary stars, this would indicate that such systems do form readily within the halo, and the lack of a significant population within globular clusters is due to the disruption of possible binaries within rich clusters and/or the inability to study the central regions of rich clusters where the blue stragglers should be concentrated.

V. SUMMARY AND CONCLUSIONS

Though accurate stellar photometry at faint magnitudes is of critical importance to a wide variety of astrophysical problems, it is a difficult goal to achieve given standard photoelectric and photographic techniques. We have tested the 16 mm blue vidicon camera at CTIO by observing the clusters NGC 2204 and E3 and have found it to be capable of providing accurate stellar photometry over an area 10 mm on a side at the f13.5 focus of the 1.5 m telescope. For a 45 minute integration, the typical uncertainty with the 1.5 m at $V = 21$ is ± 0.10 mag. The response of the camera is linear over at least 6 mag within the photometric uncertainty and showed no significant variation in slope over the entire four night run. Small variations in the zero point with time can arise from an actual variation in the response of the instrument and/or a variation in the atmospheric transmission or seeing. Clearly, it is of some value to be able to internally set the zero point for each program field.

With regard to individual clusters we have found the following:

1. The apparent distance modulus of NGC 2204 is $(m-M) = 13.40$. Combined with the reddening estimate of $E(B-V) = 0.08$ (Hawarden 1976), the cluster is estimated to be $2.5 \pm 0.3 \times 10^9$ yr old and the de-reddened turnoff has a $(B-V)_0 = 0.29 \pm 0.02$. The cluster red giant clump is at $M_v = +0.4$, brighter than that for NGC 2420 and NGC 2506. The luminosity function appears to be flat down to approximately $M_v = 6.5$, where a turnover may occur. This is similar to what is found for NGC 2420 but different from the much brighter turnover in NGC 2506. These results are consistent with a dynamical stripping mechanism operating since both NGC 2204 and NGC 2420 are found significantly farther from the Galactic plane than NGC 2506.

2. The photographic photometry of E3 by BDK suffers from rather large systematic error, primarily in the blue. Use of the photometry to calibrate the vidicon fields produced totally anomalous results for the main sequence of NGC 2204. By using the available data within NGC 2204 alone, the vidicon data were recalibrated, and the photographic photometry of BDK was transformed to the system of NGC 2204 using the stars common to the two samples. The resultant $C-M$ diagram for E3 demonstrates that the distribution of bright stars is consistent with that for a normal globular cluster, though the metallicity of the cluster is impossible to estimate at present given the sparse nature of the cluster, the photometric uncertainty in the subgiant branch, and the poor knowledge of the correct zero point for the E3 photometry. While much of the scatter present in the brighter regions of the $C-M$ diagram of BDK is removed by the present result, it is still true that the cluster contains a significant population of blue stragglers.

One final point should be made. While we feel certain that a significant error exists in the photometry of BDK, especially in the B magnitudes, it is impossible for us to state definitively where the source of the error may be. Without a direct check on the photoelectric photometry and/or a reanalysis of the photographic plates, the best we can offer are two guesses:

Variable plate response.—It has been shown in the past (McClure and Twarog 1977) that iris photometry of stars on 4 m plates suffers from significant errors for images more than $10'$ from the plate center. These systematic changes are the result of a weakening of the plate background near the outer edges of the plate and, possibly, a change in the image profile with radius. Attempts at applying corrections for such effects on iris photometry are usually crude and ineffective. In the case of BDK, the brightest stars used in the calibration are found $15'$ – $20'$ from the cluster center. While the photoelectric values for these stars may be correct, the instrumental magnitudes from the iris may be on a different system from that defined by the stars at the center of the cluster.

Incorrect color terms.—As discussed in § III, color

terms are important in transforming photographic magnitudes to the photoelectric system; they are also notoriously difficult to derive. Under the best circumstances, they require a large number of photoelectric standards over a narrow range in magnitude but a large range in color. The more common situation is that found in BDK and the present investigation, a handful of stars covering a narrow range in color, leading to large uncertainty in the color term. With photographic plates, an additional problem arises. While plates of a specific emulsion type tend to produce consistently similar color terms, the value of the color term can vary in both size and sign for different emulsions, even though the plates are technically designed to produce the same color. As an example, McClure, Forrester, and Gibson (1974) found that 103a-O plates have a B color term of $+0.07$, while Ila-O plates have a value of -0.04 . The negative slope for the Ila-O plates was confirmed by McClure and Twarog (1977) using 4 m

plates of NGC 188 from which a value of -0.09 was derived. This may be significant in that BDK derived the B magnitudes using both 103a-O and Ila-O plates but applied the same color term to both, i.e., the one equivalent to a 103a-O plate. Without knowing the relative number of emulsion types involved, it is impossible to estimate the size and direction of the effect, but, at minimum, the photometric scatter should be increased.

We are very grateful to Bruce Atwood for his help at a number of critical points in this program. B. A. T. gratefully acknowledges the financial support of McDonald Observatory which helped make this observing program possible. We also benefited greatly from discussions with Jim Hesser and Bob McClure of their photographic work on E3 which is being prepared for publication.

REFERENCES

- Atwood, B., Ingerson, T., Lasker, B. M., and Osmer, P. S. 1979, *Pub. A.S.P.*, **91**, 120.
 Bahcall, J. N., and Soneira, R. M. 1980, *Ap. J. Suppl.*, **44**, 73.
 Chiu, L.-T. G., and van Altena, W. F. 1981, *Ap. J.*, **243**, 827.
 Christian, C. A. 1980, Video Camera/CCD Standard Fields, KPNO.
 Ciardullo, R., and Demarque, P. 1977, *Trans. Yale Univ. Obs.*, **33**, 1.
 ———. 1979, in *Problems of Calibration of Multicolor Photometric Systems*, Dudley Obs. Rept. No. 14, p. 317.
 Dawson, D. 1981, *A.J.*, **86**, 237.
 Demarque, P., and McClure, R. D. 1977, in *The Evolution of Galaxies and Stellar Populations*, ed. B. M. Tinsley and R. B. Larson (New Haven: Yale University Observatory), p. 199.
 Harris, W. E., and Canterna, R. 1980, *Ap. J.*, **239**, 815.
 Hawarden, T. G. 1976, *M.N.R.A.S.*, **174**, 225.
 McClure, R. D., Newell, B., and Barnes, J. V. 1978, *Pub. A.S.P.*, **90**, 170.
 McClure, R. D., Forrester, W. T., and Gibson, J. 1974, *Ap. J.*, **189**, 409.
 McClure, R. D., and Twarog, B. A. 1977, *Ap. J.*, **214**, 111.
 McClure, R. D., Twarog, B. A., and Forrester, W. T. 1981, *Ap. J.*, **243**, 841.
 Racine, R. 1971, *Ap. J.*, **168**, 393.
 Twarog, B. A. 1978, *Ap. J.*, **220**, 890.
 ———. 1983, *Ap. J.*, **267**, 207.
 van den Bergh, S., Demers, S., and Kunkel, W. E. 1980, *Ap. J.*, **239**, 112 (BDK).
 Woolley, R., Epps, E. A., Penston, M. J., and Pocock, S. B. 1970, *Roy. Obs. Ann.*, No. 5.

JAY A. FROGEL: Cerro Tololo Inter-American Observatory, Casilla 603, La Serena, Chile

BRUCE A. TWAROG: Department of Physics and Astronomy, University of Kansas at Lawrence, Lawrence, KS 66045